A forward test of the Decelerating-Accelerating Seismic Strain model in the Mediterranean

B.C. Papazachos, G.F. Karakaisis, C.B. Papazachos, D.G. Panagiotopoulos and E.M. Scordilis

Geophysical Laboratory, University of Thessaloniki, Greece

(Received: April 11, 2008; accepted: February 13, 2009)

ABSTRACT In the last two decades several studies have shown that strong earthquakes are preceded by a sequence of smaller shocks that occur near the focal region of the mainshock with a decelerating time behaviour and by another sequence of shocks that occur in a broader region, exhibiting an accelerating mode with time. Both sequences have predictive properties expressed by empirical relations which are supported by theory. These relations form the Decelerating-Accelerating Seismic Strain (D-AS) model that allows the estimation (prediction) of the mainshock. In the present work eleven couples of such sequences are identified, which in turn probably correspond to eleven strong ($M \geq 6.3$) mainshocks ensuing in the Mediterranean area (34°N-45°N, 6°W-42°E). The time of origin, t_c, the magnitude, M, and the epicenter coordinates, $E(\varphi, \lambda)$, for each of these expected mainshocks are estimated (predicted) by the D-AS model. Model uncertainties are also provided and several statistical tests are performed in order to allow an objective forward testing and evaluation of the efficiency of the model for intermediate-term earthquake prediction, at the end of the prediction window (end of 2013).

1. Introduction

Currently applied seismic codes are almost exclusively based on seismological knowledge that only concerns the spatial distribution of seismicity. It is, however, known that seismicity varies also with time but the results of this kind of research are not considered adequate enough for a practical application. It is, therefore, a scientific and social necessity to improve existing scientific knowledge on the time variation of strong earthquake seismicity, that is, on the prediction of individual strong earthquakes.

The classical terms foreshocks - mainshock - aftershocks usually refer to the relatively short-term temporal clustering of earthquakes (of the order of weeks to months) in a relatively narrow zone close to the fault rupture which generates the mainshock and triggers aftershocks. Prediction of the next mainshock in this fault, by using properties of foreshocks, is not an easy task since foreshocks are usually small and not recognisable as such before the generation of the mainshock.

On the contrary, the terms preshocks - mainshock - postshocks, used in the present and similar works, usually refer to the relatively long-term temporal clustering of earthquakes (of the order of years) in a network of seismic faults which cover a relatively large region (of the order of a few hundreds of kilometres). The largest earthquake of this cluster, which is generated in the fault with the largest rupture, is considered as the mainshock in this region. Intermediate-term

prediction of this largest mainshock seems to be feasible because preshocks have predictive properties expressed by relations that allow the estimation (prediction) of the origin time, the magnitude and the epicentre coordinates of a such mainshock with reasonable uncertainties.

Recent research on short-term earthquake prediction (a time window of days to weeks) failed to solve this very difficult problem. Such research, however, on intermediate-term earthquake prediction (a time window of a few years), based on a wealth of observations concerning precursory seismicity patterns, seems to be a promising contribution to time-dependent seismic hazard assessment (Evison, 2001). One of the most prominent patterns is the accelerating generation of intermediate magnitude preshocks in a broad (critical) region and decelerating generation of smaller preshocks in a narrower (seismogenic) region (Papazachos *et al*., 2006b). This is a developed version of the "doughnut pattern", which consists of seismic excitation in a broad region and seismic quiescence in the narrower focal region of an oncoming mainshock (Mogi, 1969).

The time variation of precursory accelerating seismicity has been investigated by many seismologists (Tocher, 1959; Raleigh *et al*., 1982; Sykes and Jaumé, 1990; Knopoff *et al*., 1996; Brehm and Braile, 1999; Robinson, 2000; Tzanis *et al*., 2000; Papazachos and Papazachos, 2001; Papazachos *et al*., 2005, among others). This accelerating seismicity has been interpreted in terms of critical point dynamics (Sornette and Sornette, 1990; Sornette and Sammis, 1995; Rundle *et al*., 2000, 2003). Bufe and Varnes (1993) proposed the following relation for the time variation of the cumulative Benioff strain, S (in Joule$^{1/2}$), released by accelerating preshocks at the time, t:

$$S(t) = A + B(t_c - t)^m \qquad (1)$$

where t_c is the origin time of the mainshock and A, $B(<0)$, $m(<1)$ are parameters determined by the available data for each accelerating preshock sequence. Bowman *et al*. (1998) suggested the minimization of a curvature parameter, C, which is defined as the ratio of the root-mean-square error of the power-law [Eq. (1)] fitting the corresponding linear fit error and using the values of this parameter to identify regions where accelerating preshocks occur.

Intermediate-term seismic quiescence in the narrower focal region has been also observed by many seismologists (Wyss *et al*., 1981; Wyss and Habermann, 1988; Jaumé, 1992; Bufe *et al*., 1994; Zöller *et al*., 2002, among others) and has been attributed to stress relaxation due to aseismic sliding or to other causes (Kato *et al*., 1997). Other seismologists (Evison and Rhoades, 1997; Evison, 2001; Rhoades and Evison, 2006) have observed that seismic quiescence is preceded by seismic excitation in the narrower, focal region. Seismic excitation followed by seismic quiescence in the seismogenic region has been considered as a decelerating pattern of intermediate magnitude preshocks by Papazachos *et al*. (2004) who fitted Eq. (1) to the decelerating Benioff strain, $S(t)$, with $m>1$. They also used the curvature parameter, C, to identify seismogenic regions where intermediate magnitude preshocks occur with a decelerating mode (decelerating preshocks). A decelerating seismic strain can be attributed to a stress shadow expected by the Stress Accumulation Model (Bowman and King, 2001; King and Bowman, 2003).

Papazachos *et al*. (2006b), used recent reliable data from a variety of seismotectonic regimes (Mediterranean, California, Japan), to develop the Decelerating-Accelerating Seismic Strain (D-

AS) model and a corresponding algorithm for intermediate-term prediction of strong (M>6.0) mainshocks. This model, which is based on empirical relations with predictive properties, has been tested by applying it on preshock sequences of strong mainshocks that already occurred in several seismotectonic regimes. However, this backward procedure is not enough, and forward testing by attempting prediction of future mainshocks is necessary for a more objective evaluation of the predictive ability of the model.

Some attempts of such forward testing have already been made in some areas of the Mediterranean (Papazachos *et al*., 2002, 2006a), where one strong earthquake (Cythera, SW Aegean, 8 January 2006, M=6.8) was successfully predicted using this procedure (Papazachos *et al*., 2007b). Since then, however, the model has been much improved (Papazachos *et al*., 2006b) and new additional data are now available. This data can be used to improve the results of already recognized candidate regions and to identify new ones.

The purpose of the present work is to apply the D-AS model on data for shocks that occurred in the Mediterranean up to 1 October 2007. In this way, the epicenter coordinates, magnitudes and origin times of probably ensuing mainshocks are estimated to evaluate the predicting ability of the model through a forward testing procedure. Furthermore, several statistical tests and quantitative measures are provided, in order to allow an objective evaluation of the D-AS model performance after the end of the last prediction window (end of 2013).

2. The Decelerating-Accelerating Seismic Strain (D-AS) model

The D-AS model is based on Eq. (1), on empirical relations that concern accelerating seismic strain and have predictive properties and on empirical relations that concern decelerating seismic strain and also have predictive properties (Papazachos *et al*., 2006b). Most of these relations have also been derived theoretically and/or have been interpreted physically.

2.1. Accelerating preshocks

An accelerating preshock sequence follows Eq. (1) with m<1 and the relations:

$$\log R = 0.42M - 0.30\log s_a + 1.25, \quad \sigma = 0.15 \tag{2}$$

$$\log\left(t_c - t_{sa}\right) = 4.60 - 0.57\log s_a, \quad \sigma = 0.10 \tag{3}$$

$$M = M_{13} + 0.60, \quad \sigma = 0.20 \tag{4}$$

where R (in km) is the radius of the circular (critical) region, s_a (in Joule$^{1/2}$/yr $\cdot 10^4$km^2) is the rate of the long-term seismic strain, t_{sa} (in yrs) is the start time of the accelerating sequence, t_c is the origin time of the mainshock, M is the magnitude of the mainshock and M_{13} is the mean magnitude of the three largest preshocks.

A quality index, q_a, is defined by the relation:

$$q_a = \frac{P_a}{mC} \tag{5}$$

where P_a is the arithmetic mean of the probabilities that each solution obtained (M, R, t_{sa}, t_c) conforms to the global Eqs. (1), (2), (3) and (4), assuming that the deviation of each parameter follows a Gaussian distribution (Papazachos *et al*., 2002). The application of this procedure on a large sample of accelerating preshock sequences (Papazachos *et al*., 2005) resulted in the following cut-off values:

$$C \leq 0.60, \quad P_a \geq 0.45, \quad m \leq 0.35, \quad q_a \geq 3.0 \; . \tag{6}$$

Worldwide observations show that the mean value of m is 0.30, which is in agreement with theoretical considerations (Rundle *et al*., 1996; Ben-Zion *et al*., 1999) and for these reasons this value of m is adopted in the present work. The magnitude, M_{min}, of the smallest preshock of an accelerating preshock sequence for which Eq. (6) holds and where q_a has its largest value, is given (Papazachos *et al*., 2005) by the following relation:

$$M_{min} = 0.46M + 1.91 \tag{7}$$

where M is the magnitude of the mainshock. Thus, for M=6, 7, 8 the M_{min} is 4.7, 5.1, 5.6, respectively.

The geographical point, Q, for which Eq. (6) holds and the quality index, q_a, which has its largest value for a particular preshock sequence, is considered the geometrical center of the critical region, that is, the center of the circle with radius, R, given by Eq. (2). In addition to Q, there are two other distinct geographical points (V_q, P_q,) that are defined by the distribution of the epicenters of accelerating preshocks and are useful for the study of time-dependent seismicity. V_q is the geographical mean (mean latitude, mean longitude) of the epicenters of the shocks of an accelerating preshock sequence. P_q is the geographical point from where the density (number of epicenters per unit area) of accelerating preshocks decays with the distance according to a power-law and is defined as the physical center of the accelerating sequence (Karakaisis *et. al.,* 2007).

2.2. Decelerating preshocks

For a decelerating preshock sequence a power-law Eq. (1) with m>1 applies and the following relations hold:

$$\log a = 0.23M - 0.14 \log s_d + 1.40, \quad \sigma = 0.15 \tag{8}$$

$$\log\left(t_c - t_{sd}\right) = 2.95 - 0.31 \log s_d, \quad \sigma = 0.12 \tag{9}$$

where a (in km) is the radius of the circular (seismogenic) region where the epicenters of

decelerating preshocks are located, M is the magnitude of the mainshock, t_{sd} (in yrs) is the start time of the decelerating preshock sequence and s_d (in Joule$^{1/2}$/yr $\cdot 10^4$km^2) is the long-term seismic strain rate (long-term seismicity) of the seismogenic region (Papazachos *et al*., 2006b).

A quality index, q_d, has been also defined for each decelerating preshock sequence by the relation:

$$q_d = \frac{P_d m}{C} \tag{10}$$

where P_d is the mean value of the probabilities in which each one of the quantities (M, a, t_{sd}, t_c) of an obtained solution fits the global Eqs. (8) and (9), assuming that the deviation of each parameter follows a Gaussian distribution. The following cut-off values have been calculated by the use of global data (Papazachos *et al*., 2006b):

$$C \leq 0.60, \quad 2.5 \leq m \leq 3.5, \quad P_d \geq 0.45, \quad q_d \geq 3.0 \; . \tag{11}$$

From a large number of globally occurring decelerating preshock sequences an average value, equal to 3.0, has been derived for m and this value is adopted in the present work. The minimum magnitude of a decelerating preshock sequence, with the best (optimum) solution, is given by the relation:

$$M_{min} = 0.29M + 2.35 \tag{12}$$

where M is the mainshock magnitude. Thus, for M=6, 7, 8 the M_{min} is equal to 4.1, 4.4, 4.7, respectively.

The geographical point, F, for which Eq. (11) is fulfilled and where q_d has its largest, value, is considered as the geometrical center of decelerating preshocks, that is, the center of the circle that includes the epicenters of decelerating preshocks and has a radius, a (in km), given by Eq. (8). There are also two other geographical points (V_f, P_f) which are defined by the distribution of the epicenters of the decelerating preshocks. V_f is the geographical mean of the epicenters of decelerating preshocks and P_f is the physical center of the decelerating preshocks from where the frequency of these shocks decays with distance according to a power-law.

3. The data

A catalogue of earthquakes has been recently compiled for the whole Mediterranean and surrounding area (Papazachos *et al*., 2007a). This catalogue is homogeneous with respect to the magnitude of earthquakes since all magnitudes are moment magnitudes or equivalent to moment magnitudes, that is, magnitudes transformed into moment magnitudes from any other scale (i.e. M_s, m_b, published by ISC and/or NEIC) by appropriate formulas (Scordilis, 2006). The completeness of the catalogue has been defined by the traditional cumulative frequency-magnitude relation (Gutenberg and Richter, 1944) and is as follows:

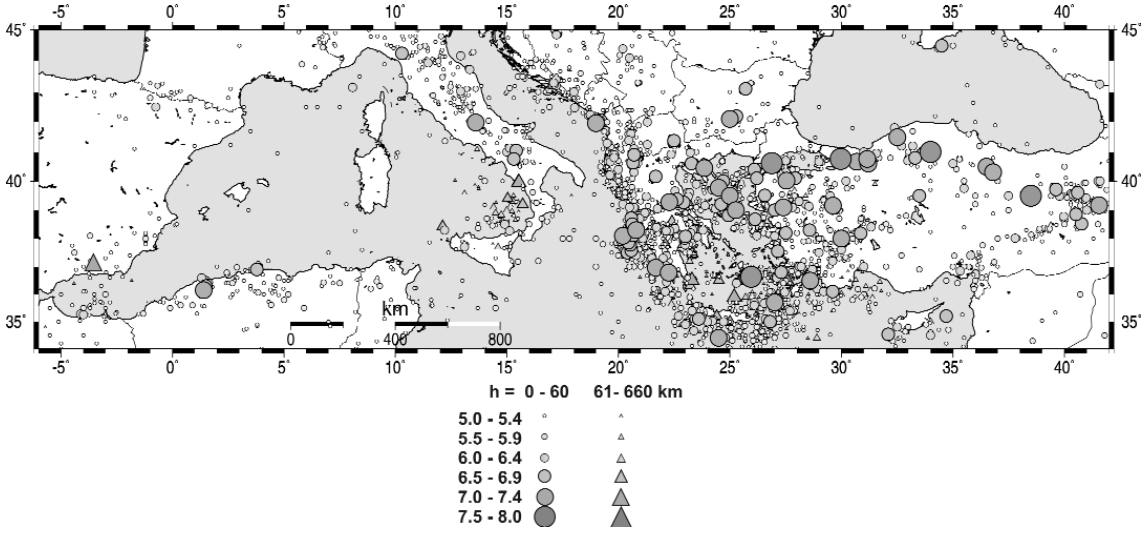

Fig. 1 - Distribution of epicenters of shocks that occurred in the Mediterranean for the period 1911-2007 with moment magnitudes $M \geq 5.0$.

$$\begin{aligned} M &\geq 5.0 \quad 1911 - 1949 \\ M &\geq 4.8 \quad 1950 - 1964 \\ M &\geq 4.5 \quad 1965 - 1980 \\ M &\geq 4.0 \quad 1980 - 2007. \end{aligned} \tag{13}$$

The uncertainties involved are up to 30 km for the epicenter and of the order of 0.3 for the magnitude. Fig. 1 shows the epicenters of the earthquakes (dots for shallow, $h \leq 60$ km, and triangles for intermediate and deep, $h > 60$ km, earthquakes) which have magnitudes $M \geq 5.0$ occurring during the time period 1911-2007.

For the purpose of the present work, four complete samples of data are needed. The first data sample concerns the mainshocks, the second sample concerns shocks of data that are used to define the long-term seismicity rates (s_a, s_d) needed in Eqs. (2), (3), (8) and (9), the third sample concerns shocks for the study of the time variation of the accelerating Benioff strain and the fourth sample concerns shocks which exhibit a decelerating time variation of the seismic strain.

Only mainshocks with $M \geq 6.3$ are considered in the present work. The main reason for this is that smaller shocks are usually associated events (preshocks, postshocks), especially in the most active parts of the Mediterranean (e.g. in the Aegean).

Long-term strain rates (s_a, s_d) for identification of critical and seismogenic regions of already occurring mainshocks have been calculated using magnitudes of earthquakes with $M \geq 5.2$ (Papazachos *et al.*, 2006b). For this reason, in the present paper, these rates have been calculated using the magnitudes of the complete sample, $M \geq 5.2$, 1911-2007, of data.

From Table 1, it is evident that all M_{min} for accelerating preshocks in relation to the corresponding start years, t_s (see the second line of each case) fulfil the completeness conditions defined by Eq. (13). It is also verified that the M_{min} for decelerating preshocks, compared to the

Table 1 - Parameters of the circular region of the decelerating seismic strain (first line) and of the circular region of the accelerating seismic strain (second line). F and Q are the geometrical centers of each region, t_c (in years) is the estimated origin time for the expected mainshock, M is its magnitude, a and R (in km) correspond to the radius of each region, C is the curvature parameter, q is the quality index, M_{min} is the magnitude of the smallest shock (preshock) considered, n is the number of these shocks, t_s is the start year of the sequence, and s (in Joule$^{1/2}$/yr·10^{4}km^2) is the long-term strain rate in each region.

	t_c	F/Q	M	a/R	C	q	M_{min}	n	t_s	logs
1	2010.7	37.7, -5.5	6.7	204	0.41	7.2	4.2	26	1974	4.47
	2013.3	36.3, -4.4	6.7	198	0.46	4.4	5.0	26	1931	4.71
2	2010.1	43.3, 2.0	6.8	245	0.23	12.2	4.2	36	1966	4.21
	2008.8	41.6, 1.4	6.9	585	0.38	3.2	5.2	47	1924	4.21
3	2010.8	44.5, 17.2	6.8	171	0.30	9.9	4.2	70	1989	5.20
	2009.0	42.8, 11.7	6.5	306	0.38	7.5	4.9	57	1964	5.17
4	2011.2	38.7, 16.2	6.6	140	0.27	9.0	4.3	28	1993	5.45
	2010.6	37.8, 18.0	6.7	259	0.37	8.3	4.9	66	1994	5.66
5	2008.4	40.8, 30.3	6.6	134	0.28	9.7	4.2	168	1994	5.78
	2008.7	38.8, 19.3	6.6	161	0.34	7.7	5.0	26	1995	6.08
6	2007.9	41.2, 23.4	7.1	173	0.43	6.2	4.3	55	1993	5.73
	2008.5	40.7, 25.4	7.0	328	0.51	5.4	5.0	75	1988	5.77
7	2011.2	36.8, 26.3	6.4	128	0.15	14.9	4.1	520	1997	5.80
	2010.6	35.8, 24.3	6.4	194	0.26	9.7	5.8	74	1986	5.63
8	2010.9	39.4, 26.5	6.3	105	0.25	11.1	4.1	260	1997	5.83
	2008.9	40.9, 26.7	6.3	154	0.43	7.1	4.7	37	1985	5.67
9	2010.1	37.8, 34.4	6.7	143	0.30	8.7	4.3	21	1992	5.46
	2009.2	36.3, 37.1	6.8	397	0.32	10.2	4.9	93	1953	5.00
10	2009.2	42.0, 33.0	7.1	180	0.45	5.9	4.4	27	1990	5.38
	2009.7	39.7, 36.8	7.0	385	0.34	9.1	5.0	82	1977	5.44
11	2008.7	41.1, 39.0	6.9	173	0.50	6.0	4.3	25	1989	5.34
	2010.6	37.8, 39.7	7.1	394	0.25	12.3	5.1	87	1976	5.37

corresponding start times of the decelerating deformation phase (see the first line for each case), fulfil the completeness conditions for the nine decelerating sequences but not for the first two sequences considered in the present work (see Table 1). However, the omission of a few small shocks in the first, excitational phase of a decelerating sequence bears no major effect on the results obtained since the largest decelerating preshocks define the excitational strain during this phase. As a matter of fact, the omission of small shocks in this phase acts against the procedure that identifies a decelerating sequence, hence any possible artificial result due to such reason is excluded.

4. The procedure followed

In order to identify currently active regions of decelerating and accelerating seismicity and estimate (predict) the corresponding probably ensuing mainshocks, the whole Mediterranean has been divided into a number of seismic zones (typically 300 km x 300 km in size) and each zone was covered by a grid of points with a certain density (e.g. 0.2°NS, 0.2°EW). A four-step procedure was applied to each zone. During the first and second steps, identification of regions of decelerating and accelerating shocks was performed and the origin time, t_c, and magnitude, M, of the ensuing mainshock are estimated (predicted). During the third step, the geographical

coordinates of the mainshock epicentre were determined (predicted), while during the fourth step the probability of a random occurrence of a mainshock, within the predicted windows, was estimated.

4.1. Identification of regions of decelerating shocks

To identify a region where decelerating shocks occur, each point of the grid is considered as the center of a circular region and the magnitudes of the shocks (decelerating preshocks) with epicenters within this region, are used to calculate the cumulative Benioff strain, $S(t)$, at the origin time of each shock, as well as the parameters of Eqs. (1), (8), (9) and (10). Calculations for each grid point are repeated for a large number of assumed values of a (in steps of 5 km), of M (in steps of 0.1), and t_{sd}, t_c (in steps of one year). All valid solutions [which fulfil Eq. (11)] are considered and the geographical point, F, with the largest value of the quality index, q_d, is taken as the geometrical center of decelerating preshocks, while the solution corresponding to this point is considered as the best solution (C, q_d, M, a, t_{sd}, $logs_d$, M_{min}, n).

Thus, a first value, M, for the magnitude of the probably ensuing mainshock is estimated by this optimization procedure. Also, a first value is calculated in this step for the mainshock origin time by Eq. (9) and by using the values of s_d and t_{sd} of the best solution. During this step the geographical coordinates of points (V_f, P_f) are also calculated by a special algorithm.

4.2. Identification of regions of accelerating shocks

The grid used in the first step is also used in this second step and a similar optimization approach based on Eqs. (1), (2), (3) and (4) is applied. All points of the grid are tested as possible centers of a critical region using Eq. (6). The geographical point which satisfies these relations and corresponds to the largest value of the quality index, q_a, is considered as the geometrical center, Q, of the circular region, where accelerating preshocks currently occur. The solution (C, q_a, M, R, t_{sa}, $logs_a$, M_{min}, n) which corresponds to this point is considered as the best solution. During this step, the geographical coordinates of the two points (V_q, P_q) are also determined.

In the second step, a second value, t_c, for the origin time of the mainshock is calculated by Eq. (3) and a third one by the relation:

$$\log\left(t_c - t_\alpha\right) = 3.11 - 0.36 \log s_\alpha, \quad \sigma = 0.07 \tag{14}$$

where t_a is the average origin time of the accelerating preshocks which occur up to three years before the generation of the mainshock. The average of the three calculated values of t_c is considered as the predicted origin time of the expected mainshock.

Also, in this second step, a magnitude that corresponds to the best solution of the accelerating preshock is estimated and this is considered as a second value of M for the expected mainshock. In addition, a third value of M is calculated by the relation:

$$M = 1.43 M_a - 0.60, \qquad \sigma = 0.24 \tag{15}$$

where M_a is the average magnitude of the accelerating preshocks, which occur up to three years before the origin time of the mainshock. The average of the three calculated values of M is considered as the predicted magnitude of the expected mainshock.

4.3. Estimation of the mainshock epicenter

The estimation (prediction) of the geographical coordinates of the epicenter of an ensuing mainshock is based on the location of the six distinct geographical points (F, V_f, P_f, Q, V_q, P_q), that are defined by the space distribution of the preshocks. This estimation is also based on the values of the quality indices (q_{de}, q_{ae}) in the mainshock epicenter, E, with respect to their values (q_{df}, q_{aq}) in the geometrical centers (F, Q) of already occurred mainshocks, as well as on the location of point, L, of the grid with the highest time independent seismicity.

The six distinct geographical points are divided into two groups. The first group is consists of three geographic points (F, V_f, P_f) which are at relatively short distances from the mainshock epicentre and their geographical mean (mean latitude and longitude) is point, D, whose the distance from the mainshock epicentre, E, is:

$$\begin{aligned} (ED) &= 0.3\text{x}(DA)+40\pm40 \text{ km} \quad , \text{ for } (DA)\leq 260 \text{ km} \\ (ED) &= 130\pm60 \text{ km} \quad , \text{ for } (DA)>260 \text{ km}. \end{aligned} \tag{16}$$

The second group consists of the other three distinct geographical points (Q, V_q, P_q) which are at relatively large distances from the mainshock epicentre and their geographical mean, A, is in a distance E, from the mainshock epicentre, which is given by the relation:

$$\begin{aligned} (EA) &= 150\pm40 \text{ km} \quad , \text{ for } (DA)\leq 230 \text{ km} \\ (EA) &= (AD)\pm100 \text{ km} \quad , \text{ for } (DA)>230 \text{ km} \end{aligned} \tag{17}$$

Eqs. (16) and (17) form the first two constraints of the mainshock epicentre.

By investigating a large number of preshock sequences, one discovers that the mainshock epicenters have a tendency to delineate along the line DA and have a symmetrical distribution with respect to this line. Thus, by considering the distances from the line DA of the epicenters which are located in one side of this line, as positive and the distances of the epicentres which are in the other side, as negative it can be found that the mean, x, of all distances is equal to zero with a standard deviation of 80 km, i.e.:

$$x = 0\pm80 \text{ km}. \tag{18}$$

This is the third constraint of the mainshock epicentre. Measures of precursory deceleration and acceleration of seismic strain have smaller values in the mainshock epicenter than in the corresponding geometrical centers (e.g. $q_{de}<q_{df}$, $q_{ae}<q_{aq}$). This has been expressed by the following relation:

$$\frac{q_{de}+q_{ae}}{q_{df}+q_{aq}} = 0.45\pm0.13 \tag{19}$$

which forms a fourth constraint for locating the mainshock epicenter.

Time independent seismicity for each grid point, expressed by the *a/b* ratio of the parameters *a* (annual) and the *b* of the recurrence relation, has been calculated and point, *L*, with the highest value for this ratio is defined. By using global data of already occurred shocks, it was observed that the distance between *L* and the mainshock epicenter is given by the relation:

$$(LD)=110\pm70 \text{ km}. \quad (20)$$

This relation is used as the fifth constraint for locating the mainshock epicenter.

Eqs. (16), (17), (18), (19) and (20) are tested for each point of a grid and five corresponding probabilities are calculated for each of these points by assuming a normal (Gaussian) distribution of the observed deviations. The average of the five probabilities is considered as the representative value for each geographical point and the point with the highest representative probability is considered as the mainshock epicenter.

5. Results

The estimated parameters (t_c, F, M, a, C, q_d, M_{min}, n, t_{sd}, s_d) of the best solution, derived from the decelerating seismic strain, are given for each of the eleven cases of Table 1 in the first line. In the same table, the estimated parameters (t_c, Q, M, R, C, q_a, M_{min}, n, t_{sa}, s_a) of the best solution (in the second line for each of the eleven cases) for accelerating seismic strain are also included. It is observed that the mean values of the curvature parameters for the eleven decelerating sequences and the corresponding accelerating sequences (C_d=0.32±0.10, C_a=0.37±0.08), are similar with the values of these parameters (C_d=0.34±0.09, C_a=0.44±0.09) calculated for already occurred globally preshock sequences (Papazachos *et al*., 2006b).

The calculated values of the origin time, t_c, and the magnitude, M, for each of the eleven expected mainshocks are listed in Table 2. In the same table, the geographical coordinates, $E(\varphi, \lambda)$, of the estimated (predicted) epicenters are given. We consider the model uncertainties as possible errors for these predictions, that is, ±2.5 yrs for the origin time of the mainshock, ≤150 km for its epicenter and ±0.4 for its magnitude, with an 80% probability if false alarms are also taken into account (Papazachos *et al*., 2006b). The total period for the generation of the 11 expected mainshocks is approximately 6 years (2008.0-2013.7), which is reasonable since the available instrumental data (1911-2007) indicates that approximately 1.5 earthquakes with $M\geq6.3$ occur annually in the area (Mediterranean) considered in the present paper, a point which is elaborated further later in the manuscript.

Figs. 2, 3 and 4 show the epicenters of decelerating (dots) and accelerating (small open circles) shocks, the circular seismogenic region (circle which includes epicenters of decelerating preshocks) and the circular critical region (circle which includes epicenters of accelerating preshocks) for three sub-areas of the examined area (Fig. 2 for the western Mediterranean, Fig. 3 for the Aegean Sea, Fig. 4 for Anatolia). The numbers (1, 2, 3, … 11) correspond to the eleven code numbers of Tables 1 and 2. The corresponding time variations of the cumulative Benioff strain for accelerating and decelerating shocks are shown on the right of each figure, along with the best-fit curves of the power-law Eq. (1) with m=0.3 for accelerating strain and m=3.0 for

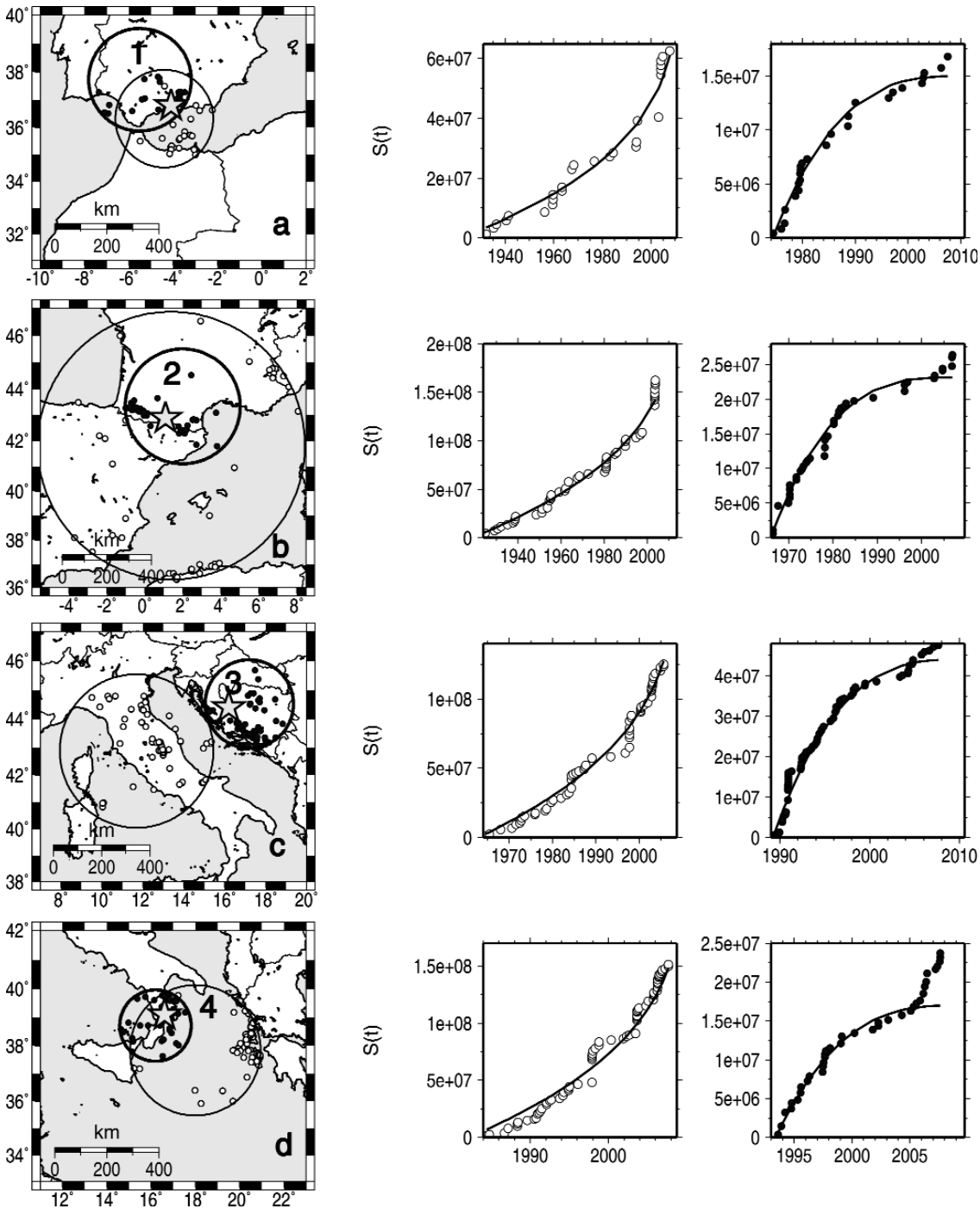

Fig. 2 - Information on the decelerating-accelerating seismicity in four regions of the western Mediterranean (a, b, c, d). Dots are epicenters of decelerating shocks (preshocks) which are included in the circular seismogenic region and small open circles are epicenters of accelerating shocks (preshocks) which are included in the circular critical region. The time variations of the accelerating and decelerating Benioff strain, *S(t)*, are shown to the right of each case. The best-fit lines of the Benioff strain time variation, which follow a power-law Eq. (1) are also shown. Numbers (1), (2), (3) and (4) correspond to code numbers of Tables 1 and 2.

Table 2 - The estimated (predicted) origin time, t_c, epicentre coordinates, $E(\varphi,\lambda)$, and magnitude, M, for each of the eleven probably ensuing mainshocks in the Mediterranean. Model uncertainties are: ±2.5 years for the origin time, ≤150 km for the epicenter, ±0.4 for the magnitude and focal depth h≤100 km for each expected mainshock, with 80% probability. The probability, P_r, for random occurrence of a mainshock with magnitude, M±0.4, during a time period of 5 years in each predicted circular region is given in the last column of the table.

	t_c	E(φ,λ)	M	Pr
1	2011.2	36.8°N, 04.1°W	6.7	0.01
2	2010.1	42.9°N, 01.1°E	6.8	0.02
3	2010.0	44.4°N, 16.2°E	6.7	0.08
4	2010.4	39.1°N, 16.6°E	6.7	0.06
5	2009.1	40.0°N, 20.5°E	6.6	0.29
6	2008.8	40.3°N, 24.4°E	7.0	0.17
7	2010.5	36.5°N, 27.0°E	6.5	0.36
8	2009.9	39.3°N, 26.9°E	6.3	0.42
9	2010.2	36.8°N, 35.3°E	6.8	0.04
10	2009.8	41.3°N, 32.6°E	7.0	0.12
11	2010.3	40.2°N, 39.0°E	7.0	0.13

decelerating strain.

In studying already occurred preshock sequences (Papazachos *et al*., 2006b), it was observed that during the last phase (~3 yrs before the mainshock) the Benioff strain deviates from the power-law [Eq. (1)], increasing strongly in decelerating, and decreasing slightly in accelerating sequences. Thus, this pattern can be considered as additional evidence for an expected mainshock to occur soon. It is interesting to notice that similar deviations are also observed in the Benioff graphs, presented in this work, for the expected mainshocks.

6. Prediction evaluation tests

In order to evaluate the reliability of the proposed predictive patterns, it is necessary to estimate the probability for the random occurrence of an earthquake within the prediction space, time and magnitude window. Such estimations are usually based on the assumption that the magnitudes of the earthquakes of the sample used are distributed according to the Gutenberg-Richter (G-R) recurrence law and their times follow a simple Poisson distribution. It is evident that if the probability for the random occurrence, in some of the eleven regions, is high compared to the D-AS model probability (80%), the corresponding predictions are practically meaningless. Hence, a reliable estimation of random occurrence probabilities is necessary for a preliminary evaluation of the proposed results.

In order to obtain reliable parameters for the G-R relation (Gutenberg and Richter, 1944) the data need to be sufficiently accurate and a large time-span has to be sampled. For this purpose, the complete samples of earthquakes M≥5.2 that occurred between 1911 and October 2007 (last date for which data were available) were used. The start time (1911) corresponds to the time from

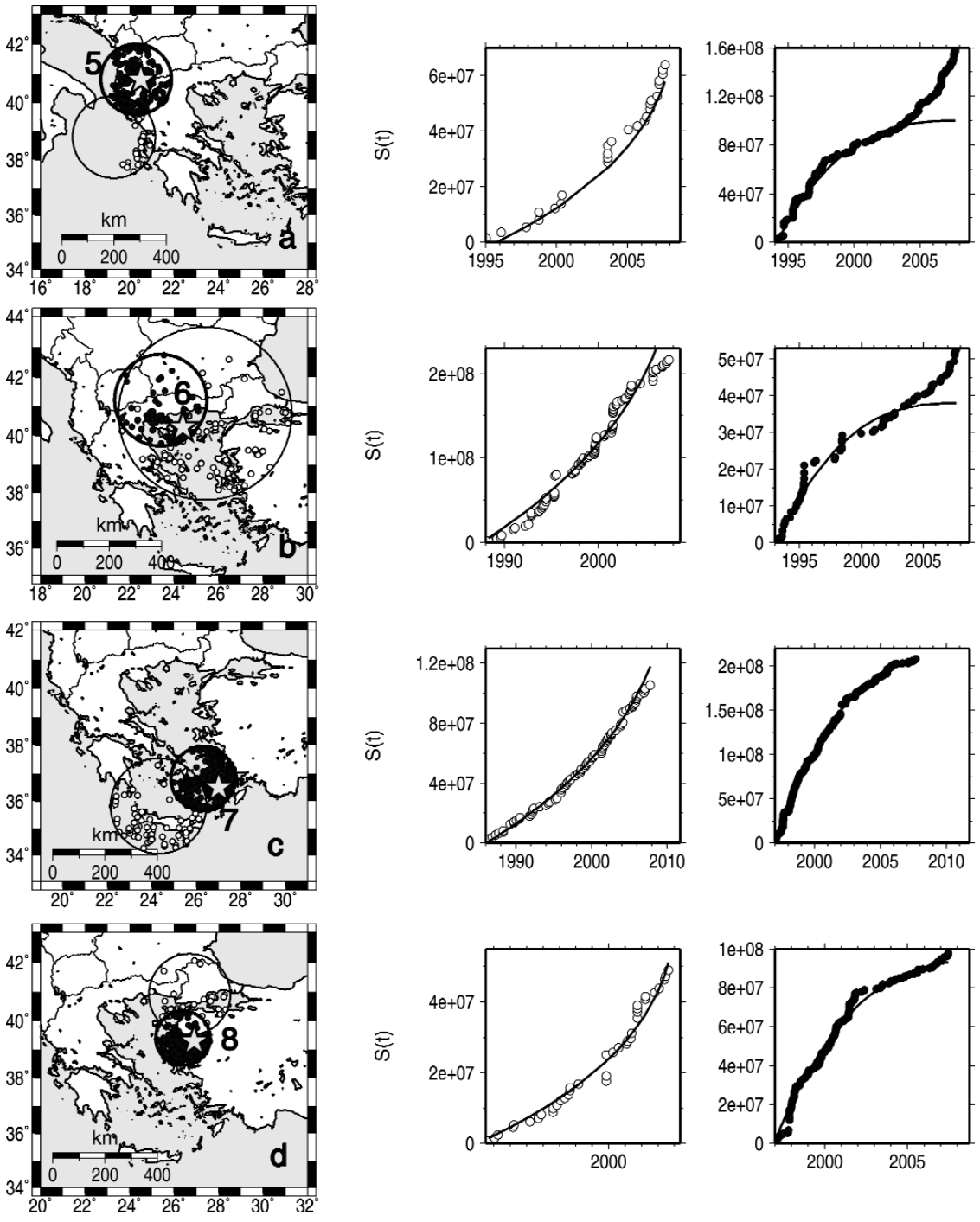

Fig. 3 - Information on the present decelerating-accelerating seismicity in the Aegean. The symbols are the same as in Fig. 2.

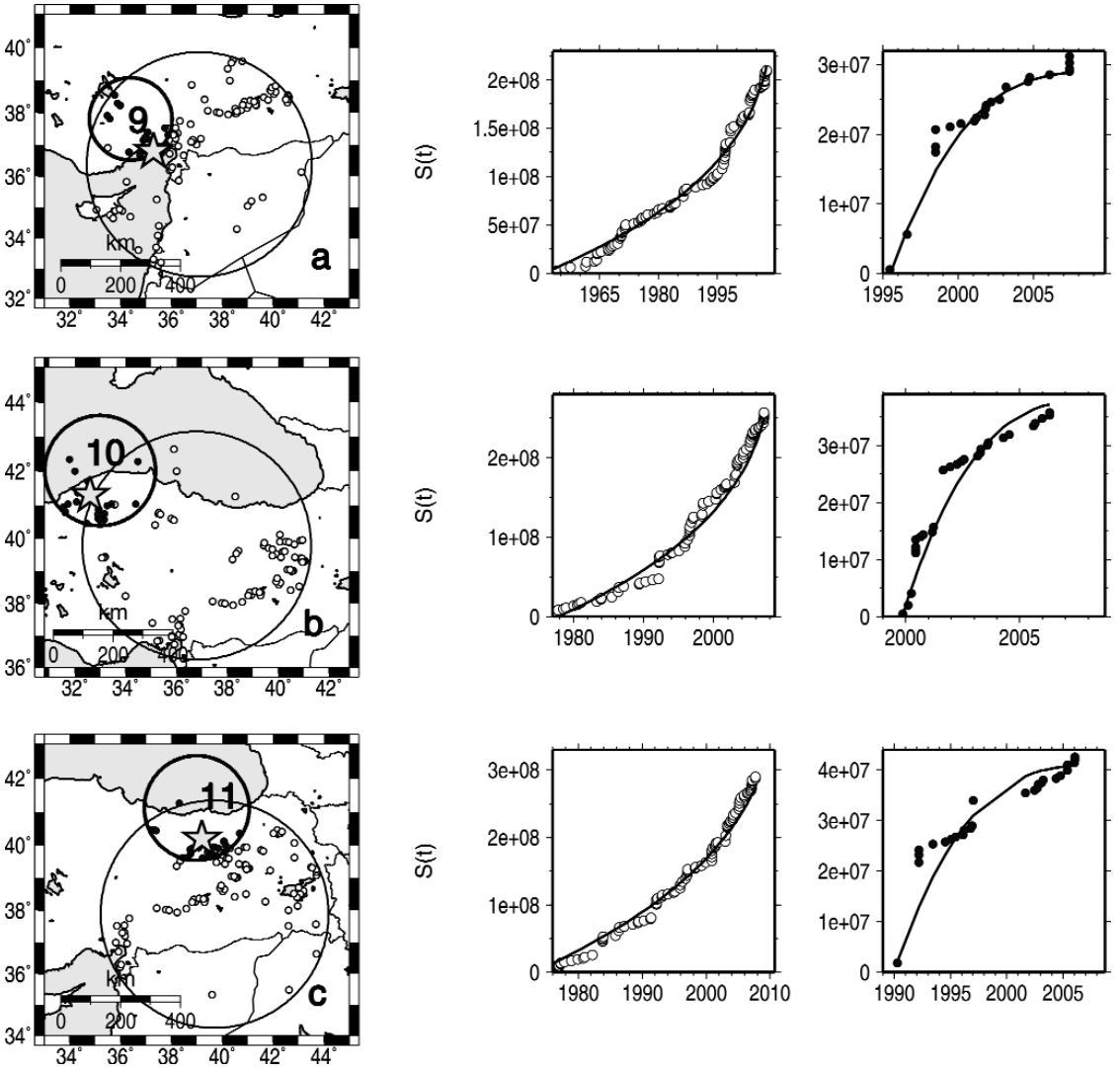

Fig. 4 - Information on the present decelerating-accelerating seismicity in Anatolia. The symbols are the same as in Fig. 2.

when several seismological stations were in continuous operation in the Mediterranean, including the Athens seismological station, which is located almost in the middle of the investigated area. The sample time interval (~97 years) covers almost the whole instrumental period and the corresponding sample size is sufficiently large (average number of sample size per year 70±50). On the other hand, the minimum magnitude (M>5.2) is sufficiently large, for all shocks considered to have been recorded by a considerable number of seismological stations, which ensures a relatively accurate location of shocks, as well as a reliable estimation of their magnitudes. Using this data set, all shallow shocks (h<100 km), in each predicted circular region (centred at the predicted epicentre and with radius 150 km), were considered and the well known G-R relation was fitted to the data in the least squares' sense:

$$logN_n = a_n - bM \quad (21)$$

where N_n is the number of shocks with magnitude M or larger, b is the slope of the line and a_n is the constant, which corresponds to 97 years' duration. Assuming a random earthquake occurrence, after reducing the line constant to its annual value ($a=a_n$ - log97), the probability, $P_{random}(M)$, for the occurrence of an earthquake with magnitude M or larger during the prediction time interval t (=5 years) is given by relation:

$$P_{random} = 1 - exp(-t/T) \quad (22)$$

where $T=10^{bM}/10^{a}$. Since the predicted magnitude window calculated by the D-AS model is $M^{Predicted}\pm0.4$, the difference of the probabilities obtained by Eq. (22) for the two magnitude limits, allows to assess the probability of a random occurrence of the earthquake in the predicted magnitude window.

It should be noted that the application of Eqs. (21) and (22) has been performed using the complete catalogue data, without any declustering of aftershocks, foreshocks, etc. However, since the probability estimates using Eq. (22) concern the high-magnitude end of the G-R curve ($6.3\leq M\leq7.0$), estimations should be considered as reliable, since very few aftershocks and practically no foreshocks have such large magnitudes in typical mainshock sequences in the Mediterranean. Furthermore, the incorporation of aftershocks and foreshocks makes the probability estimates a rather conservative (upper) estimate of the probabilities for random occurrence of a mainshock in each prediction circle.

The final probabilities of a random occurrence are listed for each prediction area in the last column of Table 2. These results show a relatively low ratio of random/D-AS model probabilities ($P_{random}/P_{D\text{-}AS}\sim0.19$), confirming the importance of the corresponding predictions. However, the probability for a random occurrence is quite large for some regions (e.g. area 8), suggesting the need for a more elaborate evaluation of the model performance, with respect to a random mainshock occurrence.

The information presented in this work allows an objective evaluation of the proposed predictions after the expiration of the estimated time windows. Such information is the time, space and magnitude windows and the corresponding probability (~0.8) for each of these eleven predictions, as well as the probabilities for a random occurrence of such mainshocks in each of the eleven regions and in the broad Mediterranean area. A simple evaluation test is the calculation of the success ratio, r, that is, the ratio of the number of successful predictions, s, to the sum, $s+n+f$, where n is the number of unsuccessful predictions and f is the number of mainshocks that occurred in the broad area (Mediterranean) outside the predicted circular regions ($r=s/[s+n+f]$). For example, in cases when none of the predicted earthquakes occurr ($s=0$), $r=0$ and when all predicted mainshocks occur in the specified prediction windows ($s=11$, $n=0$) and when no mainshock occurred outside the predicted regions ($f=0$), $r=1$. Moreover, if only five of the predicted mainshocks occur in the specified prediction windows ($s=5$, $n=6$) and two mainshocks occur in other regions of the Mediterranean area ($f=2$) the success ratio is $r=0.38$.

The simple success ratio and the random probability estimates previously described are not enough for a complete evaluation of the model performance. For example, it is not clear how to

judge the r=0.38 success ratio of the last example or how to evaluate the overall performance of the model when the random probabilities in each area (Table 2) show such a large variability. Although a large number of alternative quantitative statistical tests are available in the literature, since the prediction window (January 2008 to end of last prediction window-2013.7, i.e. 5.7 years) is relatively large, we applied a series of tests proposed by Kagan and Jackson (1995). For this purpose we have used the 11 areas where strong earthquakes are expected and separated the remaining part of the Mediterranean into 50 equal bins. Using the G-R curve for this remaining part of the Mediterranean, it is easily found that the probability of a random occurrence of a $M \geq 6.3$ within a period of 5.7 years (prediction period) is ~9.3%.

The 11 prediction areas and the 50 "background" bins correspond to 61 zones, for which we need to define the probabilities of occurrence, p_i (i=1,…61) for the two alternative hypotheses, the D-AS model and the random occurrence model. For the proposed D-AS model case and for the 5-year prediction window, we assumed that the previously mentioned probability of 80% applies within the 11 circles and the remaining 20% of events corresponded to the G-R (random) probability that an event occurs in the remaining 50 background bins, which is a reasonable choice for 20% of the cases not covered by the D-AS model. For the remaining 0.7 years of the complete examined period, we used the corresponding G-R probabilities for all zones, resulting in a final probability value for each zone. On the other hand, for the G-R (random occurrence) model, which is used as the alternative model for comparison, we have employed the corresponding G-R probabilities for the 11 prediction areas (Table 2) and the 9.3% G-R random probability for the 50 bins of the remaining (background) area.

All statistical tests are based on a large number of simulations (5000 in our case). For each simulation, a uniform, random number between 0 and 1 is drawn and compared against the reference probability p_i of each model (D-AS or random). If this number is less that the zone probability, p_i, (for each model) then the zone is considered filled (c_i=1), hence in this simulation the zone will be filled by a mainshock, otherwise it is considered empty (c_i=0) [see Kagan and Jackson (1995) for details]. It should be pointed out that the combination of D-AS probabilities (80%) for the 5-year period with the 0.7 year G-R probabilities in each of the 11 prediction areas practically did not affect the 80% probability estimate, as the corresponding G-R probabilities are quite small, with the exception of cases 5, 7 and 8 in Table 2, where the combined probability increases to ~89.2%.

Using the final set of 5000 simulations, several tests can be performed. The first test (*N*-test) examines the total number of expected mainshocks for each model. The corresponding cumulative probability curves for the two models are shown in Fig. 5a, where the D-AS and G-R models are presented with a solid and dashed line, respectively. The two curves show a small difference, as shown by the average number of earthquakes expected to 2013.7, 10.1 events for the D-AS model and 7.3 events for the random (G-R) model. Despite the apparent difference, it is interesting to note that not very different numbers of mainshock are found, although the probabilities for the individual 61 examined zones are very different for the two models. On the other hand, the estimate obtained from the D-AS model shows a slightly larger but not unrealistic number of earthquakes, since the results for the G-R model show that even scenarios which include up to 17 events are found in the simulations of the random occurence model. This result suggests that the 80% probability used for the 11 prediction areas does not lead to unrealistic assumptions and that the expected ~6 year behavior for both models is compatible with the total number of $M \geq 6.3$ events expected, with the D-

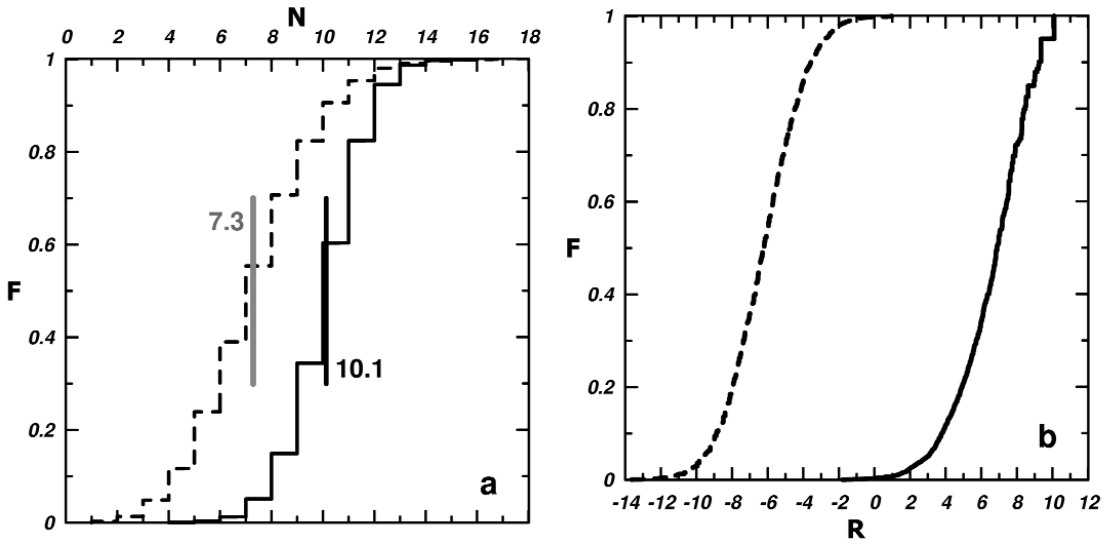

Fig. 5 - a) *N* (expected number of mainshocks) and, b) *R* (difference of log-likelihoods) cumulative curves for the simulations of the D-AS and G-R models (see text for explanation). The mean number of events expected in the next ~6 years according to each model is also shown (a). Although the *N*-curves are slightly different, a significant difference is observed for the two *R*-curves, allowing the evaluation of the performance of both models after the end of the evaluation period

AS model showing a slightly larger number of events. The slightly small bias between the two model curves of Fig. 5a suggests that it is not possible to perform a reliable discrimination of the model performance at an appropriate probability level (e.g. 90%) at the end of the examined period, if the *N*-curve is used.

The second test, called the *L*-test (Martin, 1971) estimates the logarithm of likelihood:

$$L = \sum_{i=1}^{N} c_i \log p_i + \sum_{i=1}^{N} (1 - c_i) \log(1 - p_i). \tag{23}$$

If zones with a high probability for one of the tested models (p_i>>0) are filled (c_i=1) and zones with a low probability (1-p_i>>0) are empty (c_i=0→1-c_i=0), then *L* obtains large values, showing the significance of the specific model and the corresponding probability distribution, whereas low *L* values, suggest a poor model performance. Using the results from the available simulations, the cumulative distribution of the *L* values can be examined, giving characteristic curves having an *L*-shape. Unfortunately, as in the *N*-test, both examined models (D-AS and G-R) show similar *L*-curves, hence it is also not possible to use this test for model performance comparison. For this reason, the *R*-test was used (Martin, 1971), where the difference $R=L_{D\text{-}AS}-L_{Random}$ is estimated, where $L_{D\text{-}AS}$ and L_{Random} are the computed *L* values from Eq. (23) for the two-model probability distributions (p_i, i=1,…61) of the two models.

Fig. 5b shows the two *R*-curves; one (solid line) for the D-AS model and one (dashed line) for the random (G-R) probabilities, which exhibit no overlapping even at the 95% confidence level. This

clear difference reflects the fundamental differences between the two examined models: in the 11 circular prediction areas where large earthquakes are expected according to the D-AS model, the corresponding G-R probabilities are relatively small (~19% of the D-AS model probabilities, as indicated earlier). On the contrary, for the 50 background bins, the D-AS probabilities are extremely small (20% of the corresponding G-R probability). This contrast results in a clear difference of log-likelihoods [Eq. (23)] in each zone, as these likelihoods strongly depend on the assumed probability model. This behaviour of the *R*-test makes it appropriate to evaluate the reliability of the D-AS model, as has also been demonstrated for the expected large earthquakes in central Asia (Papazachos *et al*., 2007c). Therefore, the use of the actual *R*-value for the finally, observed $M \geq 6.3$ mainshock distribution up to 2013.7 will allow the objective evaluation of the reliability of the proposed D-AS prediction, at least when comparing it to the G-R random occurrence of mainshocks.

7. Discussion

The method applied in the present work concerns the prediction of only the largest mainshock in each identified candidate region. Most of these regions include networks of faults, where other strong earthquakes, not predicted by the present method, may occur. A typical example is the recent strong mainshock activity in the southwestern part of the Hellenic arc, which included four shallow and intermediate-depth events with $M \geq 6.2$ between January 2006 and February 2008. Should such a region have more than one strong earthquake within the predicted time window (±2.5 years), space window (≤150 km) and magnitude window (±0.4), only the largest of these earthquakes can be predicted by the proposed method, as the intense seismic activity and stress re-distribution in the examined regions excludes the possibility of using seismicity measures to detect the events that follow.

It must be pointed out that the path to a successful and reliable prediction of individual earthquakes is hard and probably long and the present work is part of this effort. The predicting ability of the model will be validated after the expiration of the predicted time windows (e.g. end of 2013). Therefore, the uncertainty windows specified in the present work must be considered as indicative. The real uncertainties need to be re-examined, if the results of this forward test are clearly proven as non-random. Thus, the present work is really a test for the improvement of our current knowledge on earthquake prediction, hence, clearly, it is addressed mainly to scientists.

During the reviewing process, a strong earthquake occurred on July 15, 2008 in southeastern Greece, causing damage in the Islands of Rhodes. The earthquake parameters for this event are t_c = 2008.5, M = 6.4, E (φ=36.0ºN, λ=27.9ºE) and h = 60 km (source European-Mediterranean Seismological Centre). If we consider the parameters (and their uncertainties) for the earthquake expected in this region 7 of Table 2 [t_c^* = 2010.5 ± 2.5 yrs, M^* = 6.5 ± 0.4, E^* (φ=36.5ºN, λ=27.0ºE), with an uncertainty of ≤ 150 km, $h^* \leq 100$ km], it is clear that the specific mainshock was generated within the predicted time, magnitude, epicenter and focal depth windows. Therefore, this can be considered as a successful intermediate-term prediction for a strong earthquake. The corresponding probability for the random occurrence of a mainshock for the specific region is ~36% (see Table 2), much smaller that the 80% estimate of the D-AS model. In accordance with previous discussions, the generation of this strong earthquake in Rhodes can not exclude the possibility of the generation of strong mainshocks in the fault network of region 7, within the time prediction window.

Acknowledgments. This article benefitted from useful comments and suggestions of the Associate Editor, Lawrence Hutchings, and two anonymous reviewers, who helped to improve the manuscript. The maps were produced with the GMT software (Wessel and Smith, 1995).

REFERENCES

Ben-Zion Y., Dahmen K., Lyakhovsky V., Ertas D. and Agnon A.; 1999: *Self-driven mode switching of earthquake activity on a fault system.* Earth Planet. Science Lett., **172**, 11-21.

Bowman D.D., Quillon G., Sammis C.G., Sornette A. and Sornette D.; 1998: *An observational test of the critical earthquake concept.* J. Geophys. Res., **103**, 24359-24372.

Bowman D.D. and King G.C.P.; 2001: *Accelerating seismicity and stress accumulation before large earthquakes.* Geophys. Res. Lett., **28**, 4039-4042.

Brehm D.J. and Braile L.W.; 1999: *Intermediate-term earthquake prediction using the modified time-to-failure method in southern California.* Bull. Seismol. Soc. Am., **89**, 275-293.

Bufe C.G. and Varnes D.J.; 1993: *Predictive modeling of seismic cycle of the Great San Francisco Bay Region.* J. Geophys. Res., **98,** 9871-9883.

Bufe C.G., Nishenko S.P. and Varnes D.J.; 1994: *Seismicity trends and potential for large earthquakes in the Alaska-Aleutian region.* Pure Appl. Geophys., **142**, 83-99.

Evison F.F.; 2001: *Long-range synoptic earthquake forecasting: an aim for the millennium*. Tectonophysics, **333**, 207-215.

Evison F.F. and Rhoades D.A.; 1997: *The precursory earthquake swarm in New Zealand: hypothesis tests II.* New Zealand Journal of Geology and Geophysics, **40**, 537-547.

Gutenberg B. and Richter C.F.; 1944: *Frequency of earthquakes in California.* Bull. Seismol. Soc. Am., **34**, 185-188.

Jaumé S.C.; 1992: *Moment release rate variations during the seismic circle in the Alaska-Aleutians subduction zone.* In: Proceed. Wadati Conference on Great Subduction Earthquakes, University of Alaska, Fairbanks, pp. 123-128.

Kagan Y.Y. and Jackson D.D.; 1995*: New seismic gap hypothesis: Five years after,* J. Geophys. Res., **100**, 3943-3959.

Karakaisis G.F., Papazachos C.B., Panagiotopoulos D.G., Scordilis E.M. and Papazachos B.C.; 2007: *Space distribution of preshocks.* Boll. Geof. Teor. App., **48**, 371-383.

Kato N., Ohtake M. and Hirasawa T.; 1997: *Possible mechanism of precursory seismic quiescence: Regional stress relaxation due to preseismic sliding.* Pure Appl. Geophys., **120**, 249-267.

King G.C.P. and Bowman D.D.; 2003: *The evolution of regional seismicity between large earthquakes.* J. Geophys. Res., **108**, (B2), 2096, doi:10.1029/2001JB000783.

Knopoff L., Levshina T., Keilis-Borok V.J. and Mattoni C.; 1996: *Increased long-range intermediate-magnitude earthquake activity prior to strong earthquakes in California.* J. Geophys. Res., **101**, 5779-5796.

Martin B.R.; 1971: *Statistics for Physicists.* Elsevier, New York, 209 pp.

Mogi K.; 1969: *Some features of the recent seismic activity in and near Japan II. Activity before and after great earthquakes.* Bull. Earthquake Res. Inst. Univ. Tokyo, **47**, 395-417.

Papazachos C.B. and Papazachos B.C.; 2001: *Precursory accelerating Beebioff strain in the Aegean area.* Ann. Geofis., **144**, 461-474.

Papazachos C.B., Karakaisis G.F., Savvaidis A.S. and Papazachos B.C.; 2002: *Accelerating seismic crustal deformation in the southern Aegean area.* Bull. Seismol. Soc. Am., **92**, 570-580.

Papazachos C.B., Scordilis E.M., Karakaisis G.F. and Papazachos B.C.; 2004: *Decelerating preshock seismic deformation in fault regions during critical periods.* Bull. Geol. Soc. Greece, **36**, 1-90.

Papazachos C.B., Karakaisis G.F., Scordilis E.M. and Papazachos B.C.; 2005: *Global observational properties of the critical earthquake model.* Bull. Seismol. Soc. Am., **95**, 1841-1855.

Papazachos B.C., Karakaisis G.F., Papazachos C.B. and Scordilis E.M.; 2006a: *Perspectives for earthquake prediction in the Mediterranean and contribution of geological observations.* In: Robertson A.H.F., Mountrakis D. (ed.), Tectonic Development of the Eastern Mediterranean, Special Volume, Geological Society, London, **260**, pp. 689-707.

Papazachos C.B., Karakaisis G.F., Scordilis E.M. and Papazachos B.C.; 2006b: *New observational information on the precursory accelerating and decelerating strain energy release.* Tectonophysics, **423**, 83-96.

Papazachos B.C., Comninakis P.E., Scordilis E.M., Karakaisis G.F. and Papazachos C.B.; 2007a: *A catalogue of earthquakes in Mediterranean and surrounding area for the period 1901-2007.* Publ. Geoph. Laboratory, University of Thessaloniki.

Papazachos B.C., Karakaisis G.F., Papazachos C.B. and Scordilis E.M.; 2007b: *Evaluation of the results for an intermediate-term prediction of the 8 January 2006 M_w 6.9 Cythera earthquake in the southwestern Aegean.* Bull. Seismol. Soc. Am., **97**, 1B, 347-352, doi: 10.1785/0120060075.

Papazachos B.C., Scordilis E.M., Panagiotopoulos D.G., Papazachos C.B. and Karakaisis G.F.; 2007c: *Currently active regions of decelerating-accelerating seismic strain in central Asia.* J. Geophys. Res., **112**, doi: 10.1029/2006JB004587.

Raleigh C.B., Sieh K., Sykes L.R. and Anderson D.L.; 1982: *Forecasting southern California earthquakes.* Science, **217**, 1097-1104.

Rhoades D.A. and Evison F.F.; 2006: *The EEPAS forecasting model and the probability of moderate-to-large earthquakes in central Japan.* Tectonophysics, **417**, 119-130.

Robinson R.; 2000: *A test of the precursory accelerating moment release model on some recent New Zealand earthquakes.* Geophys. J. Int., **140**, 568-576.

Rundle J.B., Klein W. and Gross S.; 1996: *Dynamics of a travelling density wave model for earthquakes.* Phys. Rev. Lett., **76**, 4285-4288.

Rundle J.B., Klein W., Turcotte D.L. and Malamud B.D.; 2000: *Precursory seismic activation and critical-point phenomena.* Pure Appl. Geophys., **157**, 2165-2182.

Rundle J.B., Turcotte D.L., Shcherbakov R., Klein W. and Sammis C.; 2003: *Statistical physics approach to understanding the multiscale dynamics of earthquake fault systems.* Rev. Geophys., **41**, 1019-1048.

Scordilis E.M.; 2006: *Empirical global relations converting Ms and mb to moment magnitude.* J. Seismology, **10**, 225-236.

Sornette A. and Sornette D.; 1990: *Earthquake rupture as a critical point. Consequences for telluric precursors.* Tectonophysics, **179**, 327-334.

Sornette D. and Sammis C.G.; 1995: *Complex critical exponents from renormalization group theory of earthquakes: implications for earthquake predictions.* J. Phys. I., **5**, 607-619.

Sykes L. and Jaumé S.; 1990: *Seismic activity on neighboring faults as a long-term precursor to large earthquakes in the San Francisco Bay area.* Nature, **348**, 595-599.

Tocher D.; 1959: *Seismic history of the San Francisco bay region.* Calif. Div. Mines Spec. Rep., **57**, 39-48.

Tzanis A., Vallianatos F. and Makropoulos K.; 2000: *Seismic and electrical precursors to the 17-1-1983, M=7 Kefallinia earthquake, Greece, signatures of a SOC system*. Phys. Chem. Earth, **25**, 281-287.

Wessel P. and Smith W.; 1995: *New version of the generic mapping tools released*. EOS Electronic Supplement, http://www.agu.org/eoelec, 95154e.htm, posted August 15, 1995. [htp://ww.agu.org/eos_], Eos Trans. AGU, 75 (null),%%.

Wyss M., Klein F. and Johnston A.C.; 1981: *Precursors of the Kalapana M=7.2 earthquake.* J. Geophys. Res., **86**, 3881-3900.

Wyss M. and Habermann R.E.; 1988: *Precursory seismic quiescence.* Pure Appl. Geophys., **126**, 319-332.

Zöller G., Hainzl S., Kurths J. and Zschau J.; 2002: *A systematic test on precursory seismic quiescence in Armenia.* Natural Hazards, **26**, 245-263.

Corresponding author: George F. Karakaisis
Dept. of Geophysics
Aristotle University of Thessaloniki
54124 Thessaloniki (Grecce)
phone: +2310 99 8484; fax: +2310 99 8528; e-mail: karakais@geo.auth.gr